32. ^{40}Ar-^{39}Ar AGES OF LAVAS FROM THE SOUTHEAST GREENLAND MARGIN, ODP LEG 152, AND THE ROCKALL PLATEAU, DSDP LEG 81[1]

Christopher W. Sinton[2,3] and Robert A. Duncan[2]

ABSTRACT

^{40}Ar-^{39}Ar incremental heating experiments were performed on volcanic rocks recovered by drilling during Ocean Drilling Program Leg 152, southeast Greenland Margin (63°N), and Deep Sea Drilling Project Leg 81, southwest Rockall Plateau (56°N). Both of these legs drilled into thick sections of submerged lava flows, known as seaward-dipping reflector sequences, that are part of the Tertiary North Atlantic Volcanic Province (NAVP). Results show that subaerial volcanism began at the southeast Greenland Margin as early as 61−62 Ma with the eruption of continentally contaminated lavas. After an apparent hiatus, volcanism continued with the subaerial eruption of noncontaminated, mid-ocean-ridge basalt (MORB) -like lavas. A sill or flow was emplaced at 52 Ma into the sediments overlying the basement lavas at the most seaward site (918). The MORB-like lavas of the Rockall Plateau gave poor results, although the data suggest that they erupted at 57−58 Ma and may be contemporaneous with the compositionally similar oceanic lavas of Leg 152.

Compiled ages from the NAVP indicate that most of the lavas were erupted in two distinct magmatic episodes. The first occurred prior to 60 Ma with volcanism at the southeast Greenland Margin, in West Greenland, and the northwest British Isles. This early stage of widespread volcanism most likely records the arrival of the Iceland mantle plume. The second phase of magmatism began about 57 Ma with voluminous basaltic eruptions centralized along the eventual line of continental separation. Magmatism at this stage was associated with continental breakup and asthenospheric upwelling with probable thermal input from the mantle plume.

INTRODUCTION

The early Tertiary opening of the North Atlantic Ocean was accompanied by voluminous, predominantly mafic, magmatism. The remnants of lava flows and sills associated with this event, collectively known as the North Atlantic Volcanic Province (NAVP), are preserved on Greenland, the Faeroe Islands, northwestern Britain and Ireland, and on the submerged margins of the North Atlantic. The submerged lavas were originally imaged as wedges of seaward-dipping reflector sequences (SDRS) that were correlated with subaerial lava flows (Hinz, 1981). Identified SDRS have been sampled by drilling at the Vøring Plateau (Deep Sea Drilling Project [DSDP] Leg 38 and Ocean Drilling Program [ODP] Leg 104), the southwest Rockall Plateau (DSDP Leg 81), and more recently from the southeast Greenland Margin (ODP Leg 152) (Fig. 1). These studies have confirmed that the North Atlantic SDRS are composed predominantly of subaerially erupted lava flows and tuffs.

Precise crystallization ages of the North Atlantic SDRS are essential to understanding the interplay of magmatism and continental rifting, as well as the history of formation of oceanic lithosphere in the early opening of the North Atlantic. Until now, age control on the SDRS has been determined primarily by interpretation of seafloor magnetic anomaly sequences and fossil ages from sediments overlying or between lava flows. Magnetic anomaly data (Talwani and Eldholm, 1977) indicate that the Vøring Plateau SDRS are at least Anomaly 24R age (53.3−55.9 Ma, Berggren et al., 1995), consistent with the early Eocene age of the sediments overlying the lavas (Talwani, Udintsev, et al., 1976; Eldholm, Thiede, Taylor, et al., 1987). Because the biostratigraphic data can place only a minimum age on the Vøring Plateau lavas, radiometric dating of recovered lavas or examination of the fossil assemblages of any inter-lava sediment layers must be used to determine a more precise age of volcanism.

The deepest penetration of the Vøring Plateau lavas was in Hole 642E (Leg 104) where 914 m of lavas (121 flows) and volcaniclastic sediments were drilled. The lava sequence was divided into two distinct series, a reversely magnetized upper series composed of subaerially erupted, mid-ocean-ridge basalt (MORB) -like tholeiitic lavas and a lower, normally magnetized series of mixed basaltic and peraluminous andesitic lavas (Eldholm, Thiede, Taylor, et al., 1987; Schönharting and Abrahamsen, 1989). The two series are separated by a 13-m-thick horizon of finely laminated mudstones and volcaniclastic sediments. Although there is no reported fossil age for this sediment horizon, volcaniclastic sediments within the lower series lavas contain a dinoflagellate cyst assemblage that Boulter and Manum (1989) correlated with nannoplankton Zone NP9. This stage coincides with the Paleocene/Eocene boundary (Berggren et al., 1985), assigned an age of 55 Ma by the Berggren et al. (1995) time scale. However, Boulter and Manum (1989) noted that the dinocyst assemblage is similar to that seen in coal layers between the Plateau lavas on the Isle of Mull, and these have been radiometrically dated at 60.0 ± 0.5 Ma (average of four ages; Mussett, 1986). Thus, the dinocyst information may not place a precise absolute age on the lavas.

Attempts to radiometrically date the Vøring Plateau lavas have provided variable and imprecise data. K-Ar dating of DSDP Leg 38 lavas gave ages ~46 Ma (Kharin et al., 1976), much younger than the oldest overlying sediments. Rb-Sr isochrons of the lower lava series from Hole 642E are reported from two separate groups. LeHuray and Johnson (1989) used three unleached samples to produce an isochron of 57.8 ± 1.0 Ma. Taylor and Morton (1989) used five leached samples (three of which were used by LeHuray and Johnson, 1989) to calculate a five-point Rb-Sr isochron of 63 ± 19 Ma. The differing results from these two studies and the possibility that the linear array of data represent a mixing line rather than an isochron casts doubt on the accuracy and utility of the ages, although the results of LeHuray and Johnson (1989) generally agree with the fossil ages. ^{40}Ar-^{39}Ar analysis of the Hole 642E lavas is in progress and should provide more precise age constraints on the magmatic history of the Vøring Plateau.
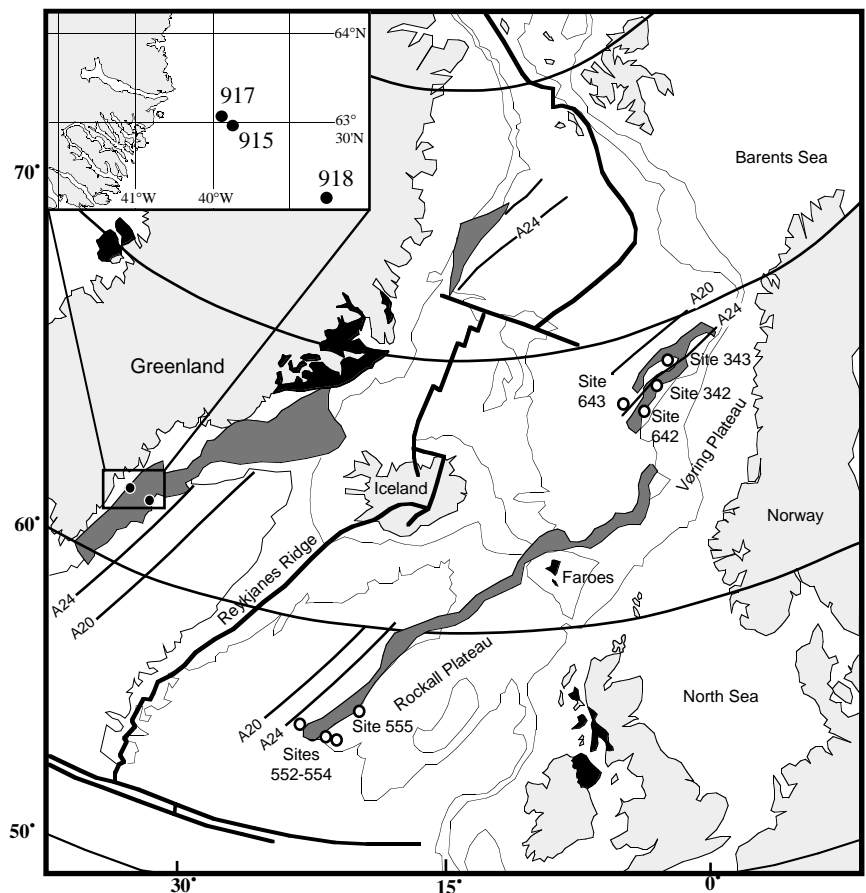
Figure 1. Map of the North Atlantic region. Shown are subaerial lava outcrops of the North Atlantic Volcanic Province (in black), seaward-dipping reflector sequences (in gray) (Eldholm and Grue, 1995; Larsen and Jakobsdóttir, 1988; White and McKenzie, 1989), magnetic anomaly lineations, and DSDP and ODP drilling sites. Previous drill sites on the Vøring margin (Legs 38 and 104) and southwest Rockall Plateau (Leg 81) are shown as open circles. The filled circles are the sites from ODP Leg 152. The inset shows detail of the Leg 152 sites.

The SDRS of the southern Rockall Plateau/Hatton Bank, which lies to the west of the British Isles, were sampled at three sites (553, 554, and 555) during DSDP Leg 81. The lavas at these sites are all consistently MORB-like in composition (Harrison and Merriman, 1984; Macintyre and Hamilton, 1984). The age of the lavas is at least late Paleocene/early Eocene based on the fossil age of the overlying sediments (Roberts, Schnitker, et. al., 1984) and identification of oceanic magnetic anomalies (Vogt and Avery, 1974). A more direct method of dating the lavas was attempted by interpreting the dinoflagellate cyst assemblages in sediments intercalated with lava flows at Site 555. These sediments, like those associated with the Vøring lavas, are correlated to Zone NP9 (Brown and Downie, 1984). K-Ar dating of the DSDP Leg 81 lavas gave a range of ages, although two from Site 555, which yielded 52.3 ± 1.7 Ma and 54.5 ± 2.0 Ma, are the most reliable according to Macintyre and Hamilton (1984).

The results from previous drilling of the North Atlantic SDRS indicate a minimum age of late Paleocene/early Eocene for the lavas of the SDRS from the eastern margin of the North Atlantic. Because the complete volcanic succession was not penetrated at any of these sites, the maximum age of the SDRS is unknown, as is the total duration of volcanism that produced the SDRS. ODP Leg 152 drilled the landward feather-edge of the SDRS at the southeast Greenland Margin, penetrating the lowermost portion of the volcanic stratigraphy at one of the sites, thus allowing the possibility of determining the age of initial volcanism at this part of the western North Atlantic Margin.

Here, we present results from ^{40}Ar-^{39}Ar incremental heating experiments on lavas recovered during ODP Leg 152 and DSDP Leg 81. The Rockall Plateau is a few hundred kilometers to the south of the margin conjugate to the southeast Greenland Margin, and it is possible that the Tertiary lavas from these two regions are complementary. The purpose of this project was to constrain the age and duration of volcanism that formed the southern North Atlantic SDRS.

The age determinations indicate that subaerial volcanism at the southeast Greenland Margin began no later than 61−62 Ma and persisted at least until a small flow or sill penetrated Eocene marine sediments at 52 Ma. A significant hiatus is evident between the initial eruption of continentally contaminated lavas and the later eruption of lavas with more oceanic affinities. The age determinations from the Rockall Plateau/Leg 81 samples are poorly constrained, yet suggest an eruption age of 57−58 Ma.

SAMPLE DESCRIPTIONS

Leg 152 drilled into the volcanic basement of the southeast Greenland Margin at three sites along a transect close to 63°N (Larsen, Saunders, Clift, et al., 1994) (Fig. 1). Two sites (915 and 917) were drilled on the landward, feather-edge of the SDRS. Here, the basement is overlain by sediments that are probably late Paleocene-early Eocene age (Larsen, Saunders, Clift, et al., 1994). Only 10 m of MORB-like tholeiitic basalt was drilled in Hole 915A, but drilling at nearby Hole 917A penetrated a succession of subaerial lavas and rare tuffs (779 m; 92 flow units) and into steeply inclined, low-grade metamorphic sediments.

The volcanic stratigraphy of Hole 917A was divided into three series: a lower series of basalts and rare picrites, a middle series of more evolved basalts and rare dacites and ash tuffs, and an upper series of thin olivine basaltic and picritic flows. Geochemical and petrographic data for the lower and middle series lavas indicate that they have been variably contaminated by the continental crust and/or lithospheric mantle (Fitton et al., this volume; Demant, this volume). The upper series shows evidence of only minor addition from the crust (Larsen, Saunders, Clift, et al., 1994; Fitton et al., this volume). The boundary between the upper and middle series is marked by a sand-

stone unit (67 cm) whereas the middle to lower series boundary is based on a change in lava compositions.

In Hole 918D, located about 80 km seaward of Site 917, 122 m of subaerial lava flows (18 flow units) was cored. The lavas are all uniformly aphyric tholeiitic basalts with MORB-like compositions (Larsen, Saunders, Clift, et al., 1994). A 12-m-thick alkalic sill or flow lies within the early Eocene sediments 9 m above the basement lavas and is the youngest volcanic unit drilled. All of the Leg 152 lavas are reversely magnetized and had been assigned to magnetic Anomaly 24R or older (Larsen and Jakobsdóttir, 1988; Larsen, Saunders, Clift, et al., 1994) Lavas from the southwest Rockall Plateau were recovered during Leg 81 at Sites 553, 554, and 555. All are aphyric tholeiitic basalts geochemically similar to MORB (Roberts, Schnitker, et. al, 1984). Sites 553 and 554 are located on the western flank of the Rockall Plateau in the Edoras Basin, whereas Site 555 is more landward, between the Hatton Bank and the Edoras Bank. Site 553 basalts were subaerially erupted and are reversely magnetized. Site 554 lavas are normally magnetized and were erupted under shallow submarine conditions. Site 555 samples are reversely magnetized and were erupted in a shallow submarine environment (Roberts, Schnitker, et al., 1984).

Samples for ^{40}Ar-^{39}Ar radiometric analysis were selected from each of the Leg 152 sites (Table 1). Where possible, selected samples were the freshest, free of vesicles and cracks, highest in primary K_2O, and the best crystallized. Because of the low K_2O and fine-grained to glassy groundmass of the Site 917A upper series lavas, they are poor candidates for dating. This problem is exacerbated by the extensive zeolite-facies alteration of these rocks (Demant, this volume). Similar problems were encountered with the basement lavas from Hole 918D. The one lava unit from Site 915 is also low in K_2O, although it is relatively fresh compared with the other low-K_2O lavas from Leg 152.

The lavas from the middle and lower series of Hole 917A are generally the freshest and have the highest K_2O contents of all the Leg 152 lavas. The Unit 35B (Sample 152-917A-23R-3, 35−39 cm) ash

tuff is obviously altered: the matrix is heavily weathered, and the plagioclase crystals are cloudy and variable in composition (Demant, this volume). On the other hand, the Unit 35D (Sample 152-917A-24R-1, 8−10 cm) tuff unit still contains vitric glass shards, and the plagioclase crystals from this layer are clear and have a consistent andesine composition (Demant, this volume). A dacite flow (Unit 55; Sample 152-917A-52R-1, 46−49 cm) near the base of the middle series was analyzed because it was the best crystallized of the recovered dacites. The two plagioclase-phyric lavas from the Site 917 lower series (Units 60 and 68; Samples 152-917A-55R-4, 4−9 cm, and 64R-2, 29−35 cm) and Site 915 (Unit 3; Sample 152-915A-24R-2, 78−84 cm) have 2- to 5-mm plagioclase phenocrysts containing abundant 10- to 20-µm melt inclusions. The stratigraphically lowest analyzed samples from Site 917 (Units 82 and 84; Samples 152-917A-83R-2, 113−118 cm, and 88R-8, 46−50 cm) come from thick (15 m and 45 m, respectively) aphyric olivine basalt flows. The Site 918 sill (Section 152-918D-94R-2) is a very fresh, holocrystalline rock with relatively high K_2O (0.57%).

Samples from Leg 81 (Rockall Plateau) were examined in thin section, and selection was based on texture and degree of alteration. All are aphyric tholeiitic basalts with <0.10% K_2O. Brief petrographic descriptions and K_2O content of the analyzed samples are listed in Table 1.

ANALYTICAL METHODS

Both whole-rock minicores, drilled from the freshest part of the sample, and feldspar separates were analyzed by ^{40}Ar-^{39}Ar incremental heating methods. Feldspars from the two ash tuffs were hand-picked after crushing. To obtain phenocryst and groundmass plagioclase separates from the basalts, samples were crushed and sieved to 0.1−0.5 mm, concentrated using a Franz magnetic separator, and checked for purity under a binocular microscope. The plagioclase separates were briefly washed with 5% HF to remove surficial alter-

Table 1. Samples from the southeast Greenland Margin analyzed by ^{40}Ar-^{39}Ar incremental heating experiments.

Core, section, interval (cm)	Unit	Series	Description	K_2O (%)	Material
152-915A-					
24R-2, 78−84	3		Plag-px-ol basalt	0.21	Phenocryst plagioclase, plagioclase-free groundmass
25R-1, 9−12	3		Plag-px-ol basalt	0.15	Whole rock
152-917A-					
17R-4, 68−73	24	Upper	Aphyric ol basalt	0.16	Whole rock, groundmass plagioclase
23R-1, 31−36	34B	Middle	Aphyric basalt	0.4	Whole rock
23R-3, 35−39	35B	Middle	Tuff	?	Feldspar
24R-1, 8-10	35D	Middle	Tuff	?	Feldspar
40R-4, 15−20	52	Middle	Aphyric basalt	0.39−0.69	Whole rock
52R-1, 46−49	55	Middle	Plag-px dacite	2.89	Whole rock
55R-4, 4−9	60	Lower	Ol-plag-px basalt	0.12	Phenocryst, groundmass plagioclase
64R-2, 29−35	68	Lower	Ol-plag basalt	0.29	Phenocryst, groundmass plagioclase
69R-2, 48−53	71	Lower	Aphyric ol basalt	0.49	Groundmass plagioclase
83R-2, 113−118	82	Lower	Ophitic ol diabase	0.25	Whole rock
88R-8, 46−50	84	Lower	Ophitic ol diabase	0.29	Whole rock
152-918D-					
94R-2, 42−47	1		Plag-cpx basalt	0.57	Whole rock
106R-2, 15−19	11B		Aphyric basalt	0.07	Whole rock, groundmass plagioclase
110R-4, 67-71	14		Aphyric basalt	0.09	Whole rock, groundmass plagioclase
81-553A-					
46-3, 116−123			Aphyric basalt	0.06	Whole rock
49-3, 65−72			Aphyric basalt	0.06	Whole rock
81-554A-					
7-3, 77−85			Aphyric basalt	0.19	Whole rock
7-4, 11−18			Aphyric basalt	0.15−0.16	Whole rock
14-1, 33−40			Aphyric basalt	0.36	Whole rock
81-555-					
69-3, 121−129			Aphyric basalt	0.04−0.11	Whole rock
90-2, 102−109			Aphyric basalt	0.07	Whole rock
95-2, 16-23			Aphyric diabase	0.09	Whole rock
96-2, 30−37			Aphyric diabase	0.09	Whole rock

Notes: K_2O values reported for each unit are from Larsen, Saunders, Clift, et al. (1994), Harrison and Merriman (1984), Joron et al. (1984), and Richardson et al. (1984). Mineral abbreviations: plag = plagioclase; px = pyroxene; ol = olivine; and cpx = clinopyroxene. ? = undetermined.

ation. The groundmass (composed of clinopyroxene, plagioclase, and Fe-Ti oxides) from a coarsely crushed (0.3–0.1 mm) fraction of Sample 152-915A-24R-2, 78–84 cm, was separated from the nonmagnetic phenocrysts in an effort to avoid inclusion-bearing plagioclase phenocrysts. All samples were ultrasonically washed in distilled water and dried. Mineral separates, wrapped in high-purity Cu foil, and the whole-rock minicores were then sealed in evacuated quartz tubes and irradiated for 6 hr at 1 MW power in the Oregon State University TRIGA reactor. The neutron flux was monitored by samples of the biotite standard FCT-3 (27.55 ± 0.12 Ma; Lanphere et al., 1990) placed at regular intervals between the samples. Calculated errors for J were between 1% and 1.5%.

Ar isotopic compositions were determined using the MAP 215-50 and AEI MS-10S mass spectrometers at Oregon State University using standard methods (Duncan and Hargraves, 1990; Duncan and Hogan, 1994). Samples were incrementally heated either by radio-frequency induction heating (MS-10S) or in a low-blank, double-vacuum resistance furnace (MAP 215–50). After corrections for background, isotopic interferences, and mass fractionation, an age for each heating step was calculated. The data for each sample were then reduced as age spectra (step age vs. percentage ^{39}Ar released). Heating step ages were integrated for plateau ages if they formed a well-defined succession of contiguous steps that are concordant within 2σ error and comprised at least 50% of the ^{39}Ar released from the sample. We calculated plateau ages in two ways (Table 2). The first follows the method of Dalrymple et al. (1987), in which step ages are weighted by the inverse of the variance. In this way, the calculated mean more closely reflects the more precisely determined step ages. A more conservative method weights each step by the proportion of the total ^{39}Ar released in that step. In the discussion, we use the results from the first method. However, there was no statistical difference (at the 2σ confidence level) of the ages determined by these two methods.

The age of each step was calculated under the assumption that the original argon composition was atmospheric (^{40}Ar/^{36}Ar = 295.5). However, it is possible that the magmas did not completely equilibrate with the atmosphere upon crystallization. For each ^{40}Ar-^{39}Ar sample, isochrons were calculated, in which a linear correlation of the step isotopic compositions (^{36}Ar/^{40}Ar vs. ^{39}Ar/^{40}Ar) provide an age (related to the slope of the regression line) and an initial isotopic composition (from the ^{36}Ar/^{40}Ar intercept). Weighted linear regressions were fitted to the data from the steps included in the age plateau, ex-

cept where noted. Replicates of Sample 917A-23R-1, 31–36 cm, were analyzed by both mass spectrometers to examine the reproducibility of the analyses and ensure that there are no systematic differences between the two instruments. The plateau and isochron ages from both samples are nearly identical and well within the 2σ standard deviation.

RESULTS

Conventional K-Ar or ^{40}Ar-^{39}Ar total fusion ages may be inaccurate because of the effects of post-crystallization alteration (radiogenic ^{40}Ar loss) and/or incomplete equilibration of the rock with an atmospheric Ar composition at crystallization ("excess" ^{40}Ar). ^{40}Ar-^{39}Ar incremental heating methods allow internal checks on assumptions of closed system behavior and initial atmospheric Ar composition through age spectrum (plateau) and isotope correlation diagrams. If a sample yields concordant plateau and isochron ages and a near-atmospheric intercept, such ages are likely to represent reliable crystallization ages (Lanphere and Dalrymple, 1978). A sample that contains excess radiogenic ^{40}Ar may yield an age plateau that is older than external constraints allow, yet have a younger isochron age and an elevated ^{40}Ar/^{36}Ar. In this case, the isochron age may be geologically meaningful, while the plateau is not. Other samples fail to provide a reliable plateau or isochron age for geological and analytical reasons.

Southeast Greenland Margin

Hole 917A

The results of the incremental heating experiments on lavas from Site 917A yield variable results, as expected from petrographic and compositional data. From the upper series, an aphyric olivine basalt flow (Unit 24; Sample 152-917A-17R-4, 68–73 cm) was considered the best sample for analysis based on thin-section observations. However, an analysis of the groundmass plagioclase from this unit yielded no age plateau and an isochron (using the linearly arrayed data points) with an age (29.4 Ma) too young given the fossil and magnetic age constraints (Fig. 2). Fortunately, the analyses from the middle and lower series lavas were much more successful.

Five samples from the middle and lower series provided concordant plateau and isochron ages and near-atmospheric initial Ar com-

Table 2. ^{40}Ar-^{39}Ar plateau and isochron age calculations from the southeast Greenland Margin, ODP Leg 152.

Core, section, interval (cm)	Material	Plateau age by $1/\sigma^2$ (Ma)	Plateau age by %^{39}Ar (Ma)	^{39}Ar (% of total)	Isochron age (Ma)	N	^{40}Ar/^{36}Ar intercept ± 1σ	SUMS/ (N-2)
152-917A-23R-1A, 31–36	Basalt	60.1 ± 0.8	60.6 ± 2.3	99	59.4 ± 2.4	8	319.4 ± 3.4	275.3
152-917A-23R-1A, 31–36	Basalt	60.8 ± 1.0	60.9 ± 24	81	60.6 ± 1.8	4	297.2 ± 7.2	0.2
152-917A-24R-1, 8–10	Feldspar from tuff	62.2 ± 0.4	62.3 ± 1.4	100	62.3 ± 1.4	16	299.7 ± 2.1	375.5
152-917A-40R-4, 15–20	Basalt	60.7 ±1.2	61.3 ± 2.0	51	60.3 ± 4.2	6	291.0 ± 16.8	452.0
152-917A-52R-1, 46–49	Dacite	61.4 ± 0.6	61.6 ± 1.4	96	61.0 ± 1.2	8	300.0 ± 0.8	7.4
152-917A-69R-2, 48–53	Groundmass plagioclase	60.4 ± 0.7	60.6 ± 1.8	97	60.3 ± 1.6	7	301.3 ± 3.3	42.6
152-917A-83R-2, 113–118	Basalt	68.2 ± 1.6	68.2 ± 2.2	72	63.3 ± 1.2	4	413.2 ± 32.2	0.6
152-917A-88R-8, 46–50	Basalt	64.1 ± 2.2	64.4 ± 3.8	82	63.3 ± 1.0	5	319.1 ± 7.6	1.0
152-918D-94R-2, 42–47	Basalt	51.9 ± 0.8	51.9 ± 1.9	97	51.9 ± 1.2	7	294.8 ± 0.8	5.1

Notes: Samples 152-917A-23R-1A, 31–36 cm, and 152-917A-23R-1B, 31–36 cm, are replicate analyses, the latter measured on the AEI MS-10S and the former on the MAP 215-50. Errors for both step age plateaus and isochrons are reported to 2σ. Ages are corrected for ^{37}Ar decay; half-life = 35.1 days. $\lambda_\epsilon = 0.581 \times 10^{-10}$ yr^{-1}; $\lambda_\beta = 4.962 \times 10^{-10}$ yr^{-1}. N = number of steps used in the isochron calculation.
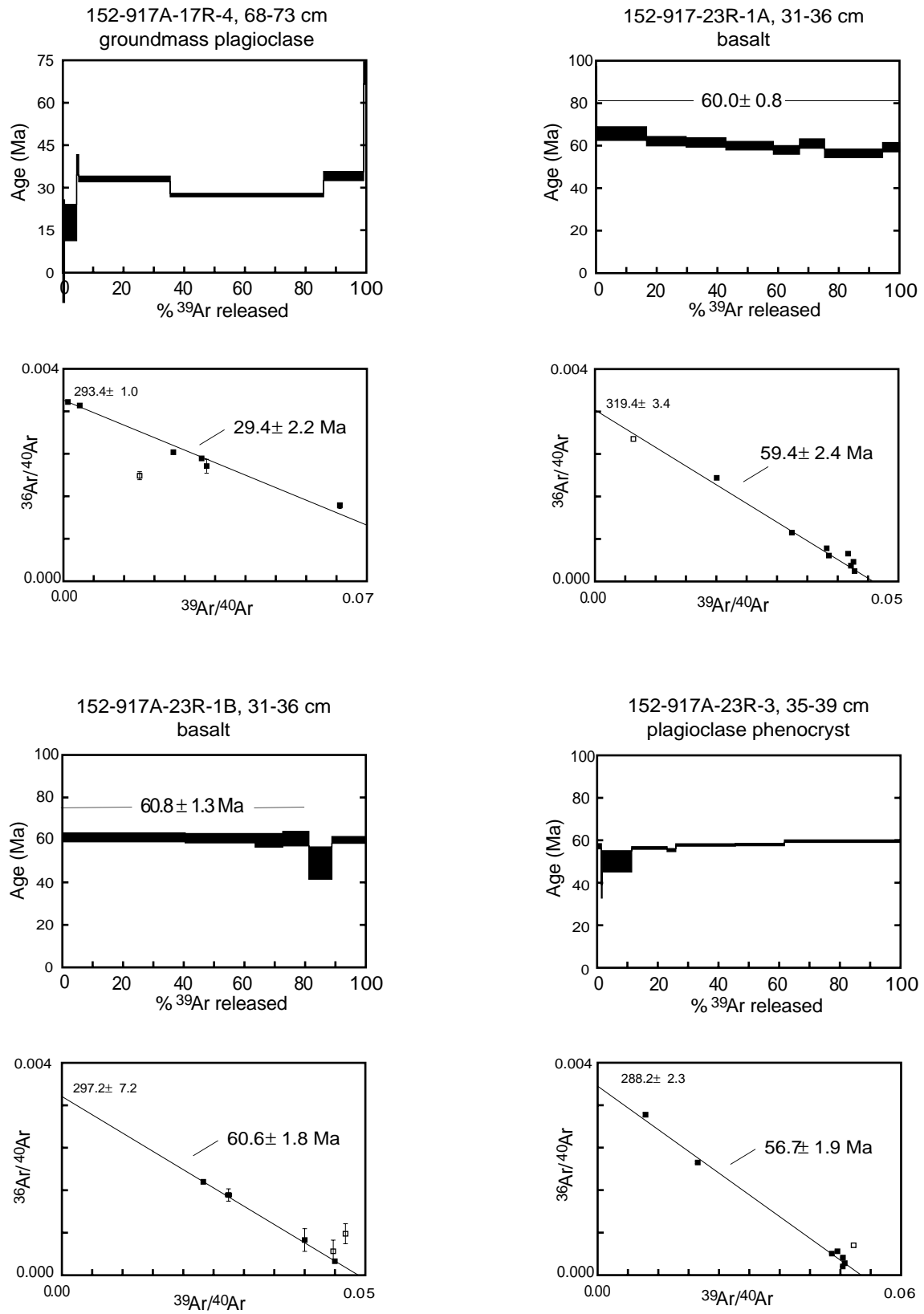
Figure 2. Step age spectra and isotope correlation diagrams from ^{40}Ar-^{39}Ar incremental heating experiments for Site 917 samples. The thickness of the bar for each step age in the age spectrum indicates the 2σ analytical uncertainty in age.

152-917A-24R-1A, 8-10 cm
feldspar

152-917B-24R-1A, 8-10 cm
feldspar

152-917A-40R-4, 15-20 cm
basalt
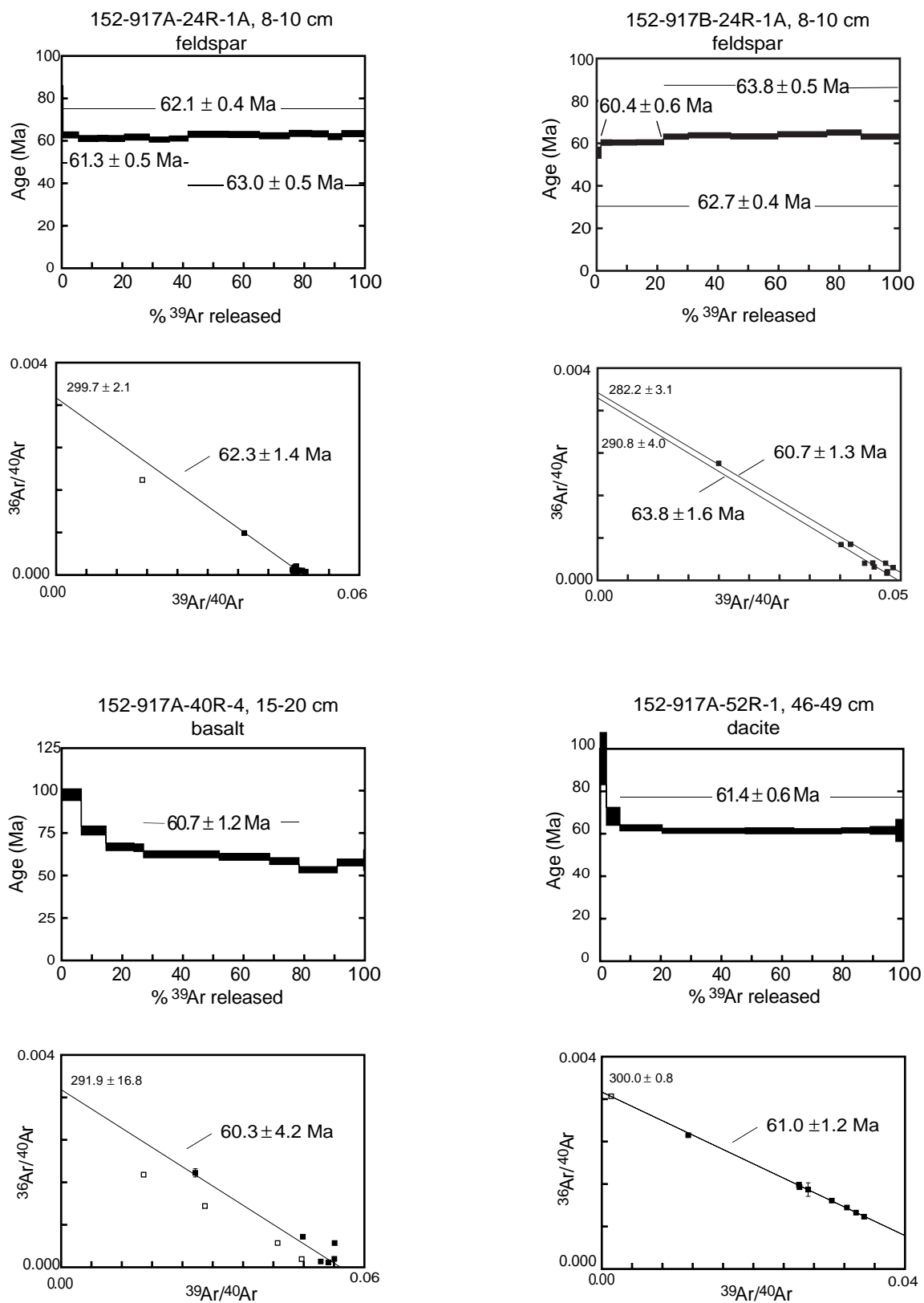
152-917A-52R-1, 46-49 cm
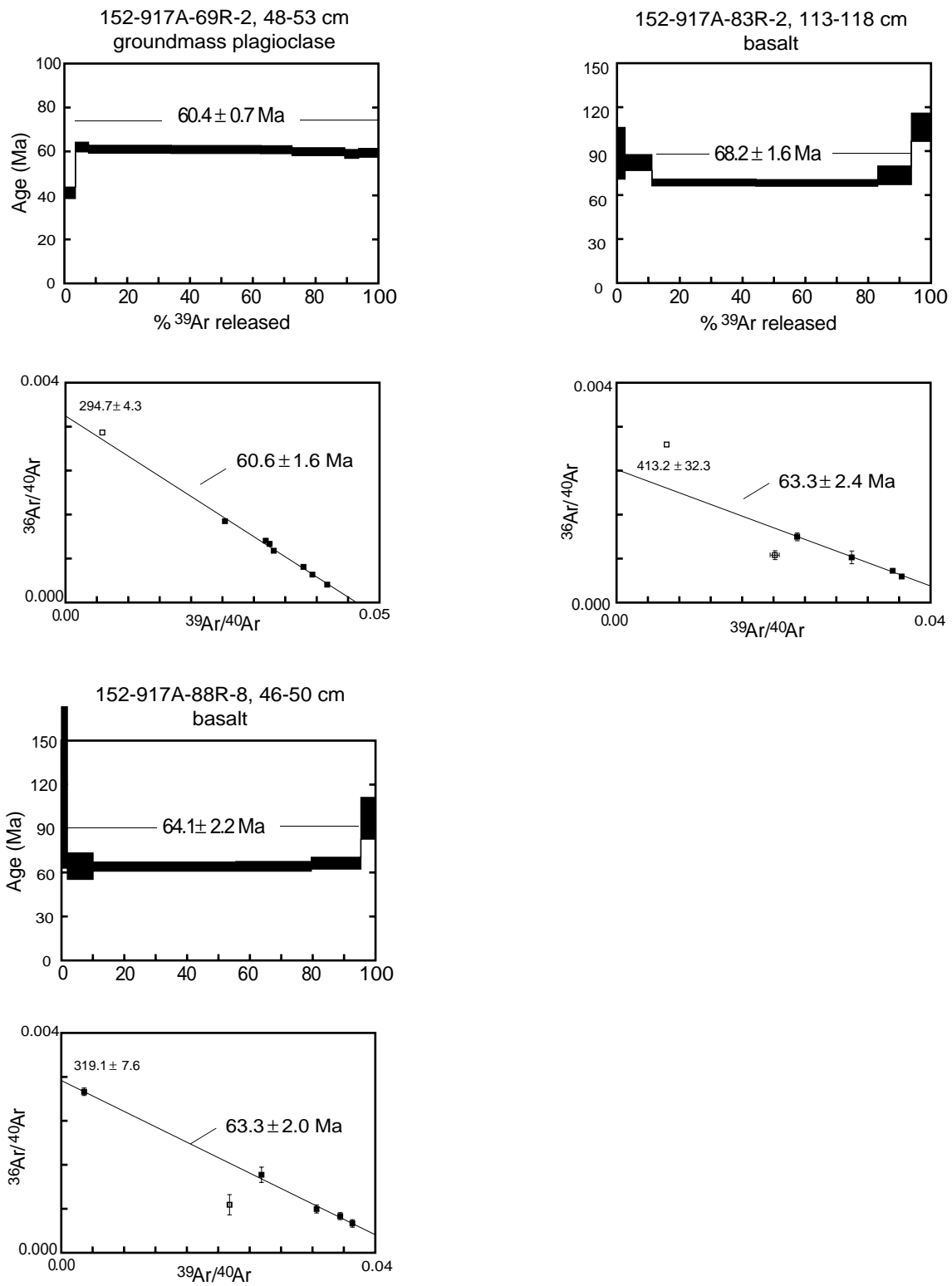dacite

Figure 2 (continued).

Figure 2 (continued).

positions (Table 1). The plateau ages range from 60.1 to 62.2 Ma, but all ages lie within 2σ analytical error. Other analyzed samples showed disturbed age spectra. The whole-rock analyses from the two stratigraphically oldest samples (holocrystalline, aphyric olivine basalts) that were analyzed (Units 82 and 84; Samples 152-917A-83R-2, 113–118 cm, and 88R-8, 46–50 cm) show evidence of excess radiogenic ^{40}Ar (Fig. 2). Both give coherent step age plateaus of 68.2 ± 1.6 Ma and 64.1 ± 2.2 Ma, respectively (Table 1). However, the saddle-shaped age spectra in which there are higher ages for the first and last few heating steps is a pattern often seen in rocks that contain excess ^{40}Ar (Lanphere and Dalrymple, 1976). This conclusion is supported by the high initial $^{40}Ar/^{36}Ar$ derived from the isotope correlation diagrams. The isochrons give identical ages (63.3 ± 2.0 and 63.3 ± 2.4 Ma, respectively) that are concordant with the more precise ages from the middle series tuff and lavas.

Another mechanism for producing a disturbed age spectrum is a loss of radiogenic ^{40}Ar or an addition of K due to alteration. This is demonstrated by the plagioclase crystals from the Unit 35B (Sample 152-917A-23R-3, 35–39 cm) ash tuff (Fig. 2), which show step ages that gradually increase with increasing temperature steps, approaching, but not reaching, the age derived from the vitric tuff (Unit 35D; Sample 152-917A-24R-1, 1–10 cm). The slightly younger age of feldspar separates from Sample 152-917A-69R-2, 48–53 cm, (Fig. 2) could be due to a small amount of radiogenic ^{40}Ar loss from alteration (evident in the lowest temperature step from the age spectrum).

Sample 152-917A-40R-4, 15–20 cm, shows a general decrease in step ages with increasing temperature. Such a pattern can be ascribed to recoil of ^{39}Ar during irradiation. We picked the middle three steps to calculate a plateau age. These three points are so tightly grouped on the correlation diagram that they do not form a linear trend, so a regression was fitted to these and two other near-colinear points. The resulting isochron is concordant with the plateau age.

The Lower and Middles Series lavas appear to have erupted without a significant time break either shortly prior to or after magnetic Chron C27n (Larsen, Saunders, Clift, et al., 1994), which suggests that the measured age range (62–60 Ma) is greater than the true period of eruption. In addition, the apparently reliable radiometric ages from Site 917 are not entirely consistent with stratigraphic position (i.e., the oldest measured ages are not from the lowermost samples) (Fig. 3). The question arises, then, which if any of the ages represents an accurate age of crystallization? The vitric ash flow tuff feldspars (Unit 35D, Sample 152-917A-24R-1, 8–10 cm) and the dacite (Unit 55, Sample 152-917A-52R-1, 46–49 cm) are the freshest and have the highest K_2O content (and are therefore the least susceptible to the effects of minor ^{40}Ar loss or gain). Given these observations, these two samples would appear to give the best crystallization ages.

The two feldspar analyses from the vitric tuff yielded the most detailed age spectra. However, these ages (62.2 ± 0.4 and 62.7 ± 0.4 Ma) are significantly older than the 60.3–60.8 Ma age range reported by Werner et al. (this volume) for feldspars from three ash tuffs (including the 24R-1 interval) in the Middle Series. In comparing the two data sets, we need to recognize some differences in the analytical techniques. The ages reported in Werner et al. (this volume) are based on laser total fusion of single crystals, whereas we used incremental heating of multicrystal samples. The advantage of the single crystal technique is that it may identify the presence of two or more age populations of crystals in the analyzed sample (such that the resulting age is a mix between the crystallization ages of the different populations). However, it cannot distinguish the effects of variable ^{40}Ar loss or excess ^{40}Ar. The advantage of the incremental heating technique is that several ages are determined for a given sample so that the several sources of ^{40}Ar within the sample (atmospheric, radiogenic, and excess) can be examined and the possibility of radiogenic ^{40}Ar loss or addition can be evaluated.

We have shown that the incremental heating results from the altered tuff feldspars from Unit 35B (Sample 152-917A-23R-3, 35–39 cm) are consistent with diffusive ^{40}Ar loss. This suggests that some
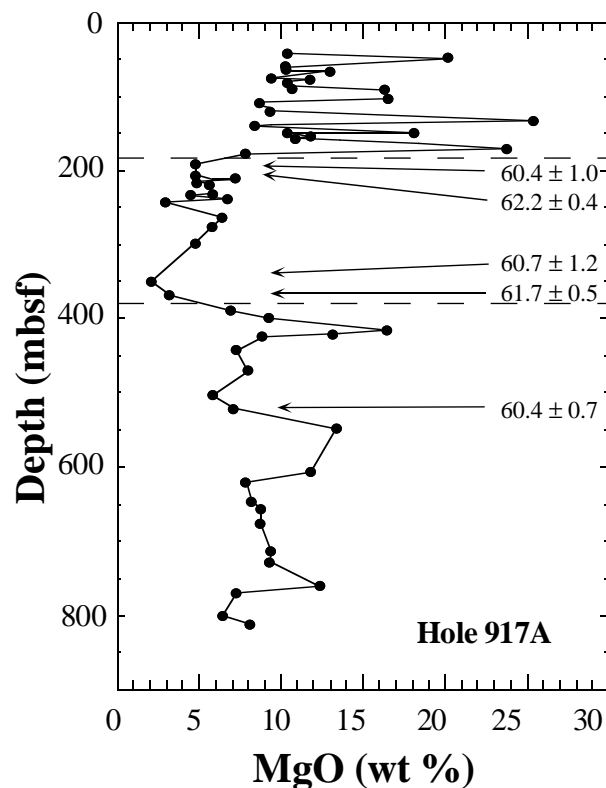

Figure 3. A plot of the MgO contents of whole-rock samples from Hole 917A (from shipboard X-ray fluorescence) and their corresponding stratigraphic positions. Note the dramatic compositional change between the Upper Series and Middle Series. ^{40}Ar-^{39}Ar plateau ages are shown (in Ma), demonstrating the inconsistency between the calculated ages and stratigraphic position.

of the single crystal ages from the altered tuffs reported by Werner et al. (this volume) may also be lower than the actual crystallization ages. Our analyses of the petrographically fresh tuff feldspars from Sample 152-917A-24R-1, 8–10 cm, do not indicate ^{40}Ar loss, so we conclude that this sample better represents the actual crystallization age. However, Werner et al. (this volume) report at least two single crystal ages from this tuff that are anomalously old (70.2 and 67.0 Ma). Although they suggest that these crystals are xenocrysts, this is not consistent with the homogeneous compositions of the feldspars (Demant et al., this volume). It is more likely that some crystals have variable amounts of excess ^{40}Ar, especially considering the evidence for crustal melting in the genesis of the Lower and Middle Series (Fitton et al., this volume; Fram et al., this volume). Upon closer inspection of our results from two replicate analyses of this sample, there is subtle evidence for a high temperature excess ^{40}Ar component. Specifically, both analyses show slightly younger age plateaus in the lower temperature steps (60.4 ± 0.6 and 61.3 ± 0.5 Ma) than in the high temperature steps (63.8 ± 0.5 and 63.0 ± 0.5 Ma), and one of the correlation diagrams shows two distinct isochrons formed by the two groups of step ages (Fig. 2). Therefore, we cannot preclude the possibility that our "bulk" plateau ages for the vitric tuff feldspars are slightly older than the actual age of crystallization, due to a small component of excess ^{40}Ar released at higher temperatures, and so the analysis of the dacite (which shows a single, unambiguous plateau) may at this time provide our most accurate crystallization and eruption age (61.4 ± 0.6 Ma). It is significant that this age is concordant with the low temperature age plateaus from the vitric tuff feldspar analyses. This age is also concordant with the 60.7 ± 0.4 (2σ) Ma age (relative to 27.55 Ma, FCT-3) for plagioclase from a dike exposed

just landward of Site 917, which has been geochemically linked with the Site 917 Lower and Middle Series (M. Storey, pers. comm.).

The 61.4 ± 0.6 Ma age for the Middle Series lavas, and their reversed magnetic polarity, is compatible with assignment to either the beginning part of the long Chron C26R or the very youngest part of Chron C27R (Berggren et al., 1995). This earliest volcanism at the southeast Greenland Margin is approximately contemporaneous with the initiation of volcanic activity in West Greenland (Storey et al., in press; Chalmers et al., 1993) and the British Isles (Pearson et al., 1996).

Hole 915A

Two samples from the one unweathered lava flow unit (Unit 3) of Hole 915A were analyzed. Plagioclase phenocrysts from Sample 152-915A-24R-2, 78–84 cm, yielded a disturbed step age spectra with anomalously old ages (Fig. 4). The old step ages could be due to magmatic ^{40}Ar released from the melt inclusions in the plagioclase, coupled with the low K_2O content (and therefore low radiogenic ^{40}Ar) of the crystals. Because of the low radiogenic ^{40}Ar, even small amounts of excess ^{40}Ar can affect the calculated age. This interpretation assumes that the melt inclusions did not re-equilibrate with atmospheric Ar and retained a magmatic Ar composition.

Similar patterns are seen in the analyses of inclusion-bearing plagioclases from Hole 917A (Units 60 and 68; Samples 152-917A-55R-4, 4–9 cm, and 64R-2, 29–35 cm). The age spectra from all these samples do not show the saddle shape that the whole-rock samples from the base of the Hole 917A lower series display. Rather, the spectra show discontinuous step ages that do not form a coherent age plateau. This difference could be due to the variable release of Ar from the melt inclusions throughout the step heating. An isochron calculated from the Sample 152-915A-24R-2, 78–84 cm, isotope correlation diagram gives a poorly constrained age that is within the range expected from the lavas (55.4 ± 14.0 Ma). However, the scatter in the data points used in the linear regression resulted in a high uncertainty for the calculated age. The phenocryst-free groundmass from Sample 152-915A-24R-2, 78–84 cm, did not show any evidence of excess ^{40}Ar, but a coherent age plateau was not generated. The linear array of the data on a correlation diagram is dispersed and does not give an isochron. Similarly discordant results were obtained from a whole-rock analysis of Sample 152-915A-25R-1, 9–12 cm (Fig. 3).

Hole 918D

A whole-rock analysis of the Hole 918D sill (Unit 1; Sample 152-918D-94R-2, 42–47 cm) gave excellent results (Table 2) with identical plateau and isochron ages (51.9 ± 0.8 Ma and 51.9 ± 1.2 Ma). However, no meaningful results were derived from the whole-rock and groundmass plagioclase analyses of the two deeper basement lavas that were analyzed. The whole-rock analysis of Unit 11B (Sample 152-918D-106R-2, 15–19 cm) displayed scattered step ages that reflect an excess ^{40}Ar component (Fig. 5). The groundmass plagioclase from this sample contained large proportions of atmospheric ^{40}Ar, leading to imprecise ages (plateau age of 46.0 ± 5.0 Ma and an apparent isochron age of 35.3 ± 4.9 Ma). However, these ages are too young given the constraint placed by the age of the overlying sill, and the young ages could be due to the effects of alteration.

Analyses of whole-rock and groundmass plagioclase from Unit 14 (Sample 152-918D-110R-4, 67–71 cm) yield scattered age spectra (Fig. 5). The whole-rock analysis does not yield a coherent age plateau, though a combined total fusion (TF) age (54.7 ± 1.8 Ma) gives an age that is plausible given the age of the overlying sill. The groundmass plagioclase did not yield a coherent plateau either, although the second step, which had ~45% of the total ^{39}Ar released, has an age of 52.6 ± 2.0 Ma. Isochrons from both the whole-rock and groundmass plagioclase can be made from steps that fall in a linear array. However, the resulting ages are too young. In summary, no reliable age information has been obtained from the basement lavas at Site 918.

Rockall Plateau/Hatton Bank

Hole 555

Two of the whole-rock analyses from Hole 555 gave reliable but imprecise ages (Table 3). Sample 81-555-69-3, 121–129 cm, revealed a good four-step plateau age of 57.6 ± 1.3 Ma and a concordant but imprecise isochron age of 51.6 ± 9.0 Ma. Sample 81-555-90-2, 102–109 cm, gave similar results (plateau 57.1 ± 5.6 Ma; isochron 56.0 ± 5.4 Ma) but less a precise plateau age due to much higher concentrations of atmospheric ^{40}Ar (Fig. 6).

Hole 553A

The whole-rock analyses from Hole 553A show disturbed age spectra (Fig. 6). Sample 81-553A-46-3, 116–123 cm, had one large step containing about 70% of the total ^{39}Ar released that has an age of 55.0 ± 2.2 Ma. An isochron made from a regression of four of the roughly linearly aligned data points gave an age of 56.5 ± 1.4 Ma, although the initial ^{40}Ar/^{36}Ar intercept (216.1 ± 33.0) is well below the atmospheric ratio, due to the analytical artifact of decreasing age with increasing temperature. These ages may be approximately correct given the age of the intercalated sediments at Site 555 but cannot be considered reliable without further corroboration. Sample 81-553A-49-3, 65–72 cm, gave discordant plateau and isochron ages of 68.5 ± 5.1 Ma and 38.4 ± 9.6 Ma, respectively.

Hole 554A

The whole-rock analyses from Hole 554A demonstrated very disturbed age spectra and no isochron information. The steady decrease in the step ages with increasing temperature is probably due to the effect of ^{39}Ar and ^{37}Ar recoil and redistribution during irradiation. In a fine-grained, multimineralic matrix, ^{39}Ar can be expelled from higher K_2O, lower temperature sites into adjacent lower K_2O, higher temperature sites (and ^{37}Ar from higher to lower CaO sites). This will result in an age spectrum that displays progressively younger ages with increasing temperature, such as that seen in Sample 81-554A-7-4, 11–18 cm (Fig. 6).

DISCUSSION
Southeast Greenland Margin

The results from the ^{40}Ar-^{39}Ar incremental heating experiments show that initial volcanism at the studied portion of the southeast Greenland Margin began by 61–62 Ma with the eruption of continentally contaminated lavas and tuffs. However, because no reliable ages were obtained from the Site 917 upper series lavas, the Site 915 lavas, or the Site 918 basement lavas, the complete magmatic history of the area must be constrained indirectly. The 61–62 Ma age of initial volcanism places a maximum age on these intermediate lavas, whereas the 52 Ma age sill at Site 918 is a minimum. What is unknown is whether or not magmatism was continuous between 62 and 52 Ma or if there were significant breaks in volcanism. The sediment horizon that separates the Site 917 middle series and upper series represents a hiatus, but of unknown duration. The change from evolved, continentally contaminated basalts and dacites to slightly contaminated, more "oceanic" olivine basalts and picrites (Fitton et al., this volume) also suggests a significant discontinuity. Such a change in volcanism may have required a dramatic change in the configuration of the mantle melting environment and magmatic plumbing system. However, without precise ages for the Site 917 upper series lavas, the duration of the hiatus remains unknown.

The Sites 915 and 918 basement lavas have MORB-like compositions with no evidence of crustal contamination (Fitton et al., this
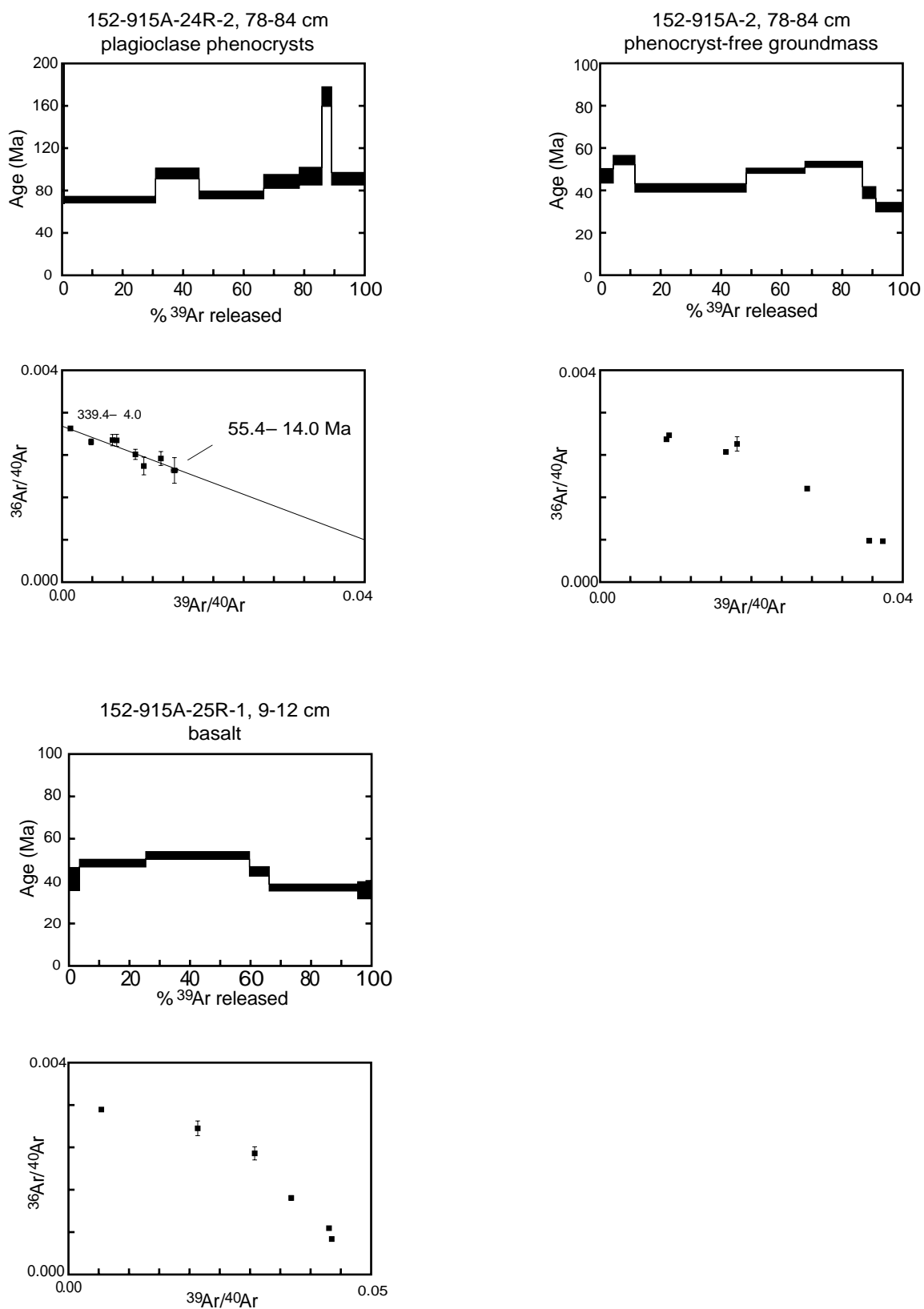
Figure 4. Step age spectra and isotope correlation diagrams from ^{40}Ar-^{39}Ar incremental heating experiments for Site 915 samples. The thickness of the bar for each step age in the age spectrum indicates the 2σ analytical uncertainty in age.

152-918D-94R-2, 42-47 cm
basalt

51.9 ± 0.8 Ma

% ^{39}Ar released

294.8 ± 0.8

51.9 ± 1.2 Ma

^{39}Ar/^{40}Ar

152-918D-106R-2, 15-19 cm
groundmass plagioclase

46.0 ± 5.0 Ma

% ^{39}Ar released

298.6 ± 3.9

35.3 ± 4.9 Ma

^{39}Ar/^{40}Ar

152-918D-110R-4, 67-71 cm
basalt

TF age = 54.7 ± 1.8

% ^{39}Ar released

318.9 ± 1.8

51.9 ± 1.2 Ma

152-918D-110R-4, 67-71 cm
groundmass plagioclase

% ^{39}Ar released

312.5 ± 11.3

47.0 ± 7.6 Ma

Figure 5. Step age spectra and isotope correlation diagrams from ^{40}Ar-^{39}Ar incremental heating experiments for Site 918 samples. The thickness of the bar for each step age in the age spectrum indicates the 2σ analytical uncertainty in age.
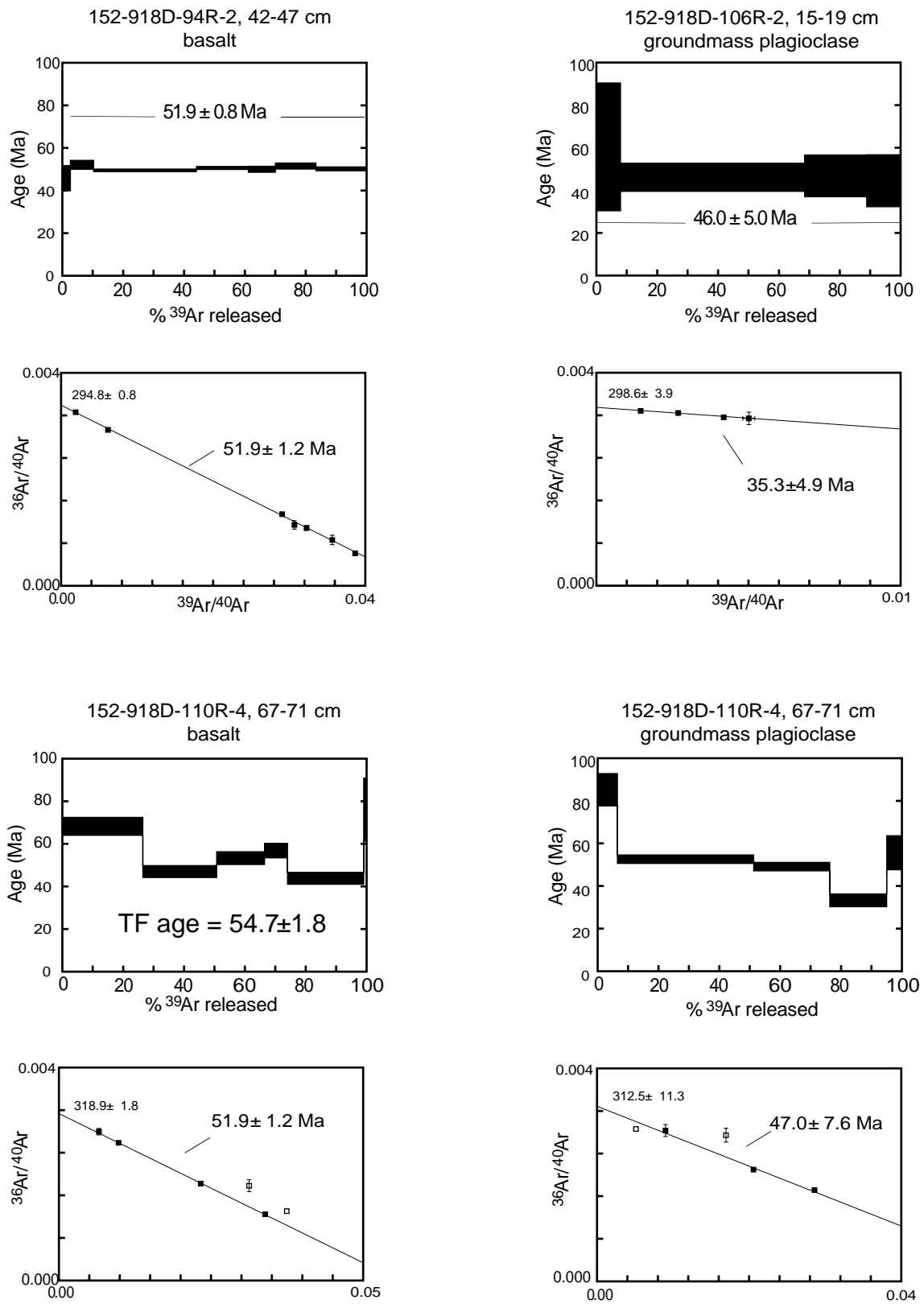
Table 3. ^{40}Ar-^{39}Ar plateau and isochron age calculations from the Hatton Bank, DSDP Leg 81.

Core, section, interval (cm)	Material	Plateau age by $1/\sigma^2$ (Ma)	Plateau age by %^{39}Ar (Ma)	^{39}Ar (% of total)	Isochron age (Ma)	N	^{40}Ar/^{36}Ar intercept ± 1σ	SUMS/ (N-2)
81-555-69-3, 121–129	Basalt	57.6 ± 1.3	58.1 ± 2.4	82	51.6 ± 9.0	4	365.2 ± 10.8	2.8
81-555-90-2, 102–109	Basalt	57.1 ± 5.6	56.7 ± 11.3	88	56.0 ± 5.4	3	300.2 ± 9.7	0.5

Notes: Errors for both step age plateaus and isochrons are reported to 2σ. Ages are corrected for ^{37}Ar decay; half-life = 35.1 days. $\lambda_\epsilon = 0.581 \times 10^{-10}$ yr^{-1}; $\lambda_\beta = 4.962 \times 10^{-10}$ yr^{-1}. N = number of steps used in the isochron calculation.

volume). If these reversely magnetized lavas represent the main part of the SDRS, they may have erupted within Chron 24R (Larsen, Saunders, Clift, et al., 1994; 53–56 Ma, Berggren et al., 1995), as long as 5 m.y. after the eruption of the Site 917 lower and middle series lavas. The last magmatic event in this part of the southeast Greenland Margin was the formation of the Site 918 sill at 52 Ma. This age is consistent with the early Eocene age (55–51 Ma) of the surrounding sediments (Larsen, Saunders, Clift, et al., 1994). The sill, therefore, places a minimum on the age of submergence.

Rockall Plateau/Hatton Bank

The Leg 81 samples all show disturbed spectra and imprecise ages. Taken together, the results from the two Site 555 lavas and the large age step from one of the Site 553 samples indicate a general eruption age of 55–58 Ma for the southwest Rockall Plateau lavas. These ages are slightly older than the K-Ar ages (52.3 ± 1.7 Ma and 54.5 ± 2.0 Ma) reported by Macintyre and Hamilton (1984). As previously mentioned, the Rockall Plateau lavas have MORB-like compositions (Harrison and Merriman, 1984; Macintyre and Hamilton, 1984), similar to the Sites 915 and 918 lavas, and can be grouped as an oceanic series. Because we have been unable to obtain reliable radiometric ages from the Leg 152 oceanic series, we tentatively assign these lavas to the period 58–57 Ma based on the compositional similarities to the Rockall lavas.

North Atlantic Volcanism

The new radiometric ages can be used to better assess the timing of volcanic events associated with the opening of the North Atlantic. In the following section, the new ages are compared to published ages for other NAVP localities. However, one should bear in mind some potential problems with such a comparison. First, there is a notable lack of reliable radiometric ages for many of the localities. Many of the K-Ar ages show a wide range as a result of alteration and excess ^{40}Ar (e.g., Noble et al., 1988). Comparison of the radiometric ages to age estimates derived from fossil assemblages can be problematic. The numerical age assigned to a specific fossil zone depends on the time scale that is used. In addition, some of the fossil ages are based on dinoflagellate assemblages correlated to calcareous nannoplankton (NP) zones, which are then in turn correlated to an absolute age scale. This chain of correlations can add significant uncertainty to the accuracy of the age estimate. In this section, the Berggren et al. (1995) time scale is used.

The 61–62 Ma initial age of volcanism for the southeast Greenland Margin is equivalent to the fossil ages derived from sediments between the stratigraphically oldest lavas in West Greenland (Larsen et al., 1992) (Fig. 7). Initial volcanism in West Greenland was characterized by the eruption of picritic lavas (the Vaigat Formation; Larsen et al., 1992). A nannoplankton assemblage in sediments near the base of the Vaigat Formation corresponds to Zone NP3 (Fig. 7; Perch-Nielsen, 1973; Jürgensen and Mikkelsen, 1974, as cited in Larsen et al., 1992). Dinoflagellate assemblages in sediments associated with the lowest lithostratigraphic member of the Vaigat Formation are interpreted to range in age from latest early Paleocene to early late Paleocene (60–61 Ma; Larsen et al., 1992). Radiometric ^{40}Ar-^{39}Ar ages of some of the earliest lavas from the British Tertiary Province (Isles of Mull, Muck, and Eigg) are 60–62 Ma (Musset et al., 1988; Pearson et al., 1996). Thus, initial NAVP volcanism occurred in at least three widespread regions (and maybe more) prior to 60 Ma.

Continental breakup and active plate separation in the North Atlantic occurred well after the initial pulse of magmatism. Seafloor spreading is recorded to have begun by Anomaly 24R (53–56 Ma, Berggren et al., 1995) and thus postdates the initial volcanic episode by about 4–5 m.y. Continental breakup occurred simultaneously with magmatism that was centralized along the present margins of the North Atlantic. SDRS lavas associated with this event include the oceanic series from Leg 152, the Leg 81 (Rockall Plateau) lavas, and the Hole 642E (Vøring Plateau) lavas. Subaerially exposed lavas on East Greenland also erupted during the second magmatic episode. The Scoresby Sund area lavas have been radiometrically dated by ^{40}Ar-^{39}Ar incremental heating methods at 56.7 ± 4.3 Ma (2σ error) (Hansen et al., 1993). The most reliable K-Ar ages from the lavas near Kangerlussuaq indicate an eruption age of 56–54 Ma (Noble et al., 1988). To the north of Kangerlussuaq between 73° and 74°N, lavas from the lower part of the volcanic stratigraphy have ^{40}Ar-^{39}Ar ages of 58–57 Ma (Upton et al., 1995).

A compilation of the new radiometric ages presented here, published NAVP lava ages, and fossil ages of ash layers in sediments in the North Sea (Knox and Morton, 1988; Morton et al., 1988) indicate that the bulk of the province is the product of two distinct pulses of magmatism, one occurring prior to 60 Ma and the other beginning around 57 Ma (Fig. 7). Although there are reported radiometric ages for intrusions formed during the interval between the two pulses (Mussett et al., 1988), their total volume is relatively minor.

In a pre-drift reconstruction of the North Atlantic (e.g., White, 1992), the initial eruptions occurred up to 2000 km apart. The synchronous formation of the lavas requires a mechanism that induces simultaneous volcanism over a wide area and can produce the high temperature, picritic melts that are observed in West Greenland and in the Site 917 lower series. In addition to being broadly distributed, these early volcanic rocks were erupted in different tectonic settings: West Greenland was adjacent to the opening northern Labrador Sea (Chalmers, 1991), southeast Greenland was situated in a previously stable cratonic region (Bridgewater et al., 1976), and the British lavas were erupted into Mesozoic rift basins (Thompson and Gibson, 1991). The widespread initial volcanism from at least these three localities may have been the result of the arrival of the Iceland mantle plume.

A plume impact model (Richards et al., 1989) is one of several geodynamic models for the NAVP that features a central role for the Iceland mantle plume. In this model, the arrival of the Iceland plume head at the base of the lithosphere resulted in widespread volcanism. Another model (White and McKenzie, 1989) proposes that volcanism was promoted by lithospheric thinning, which allowed upwelling and decompression melting of asthenosphere previously heated by the "incubated" mantle plume. According to the latter model, the earliest widespread volcanism in West Greenland and the British Isles is attributed to localized rifting when the mantle plume arrived. However, if volcanism at 62–61 Ma were driven by localized lithospheric extension, it is improbable that an area in a previously formed extensional environment (West Greenland) would experience volcanism at the same time as an area of thick, Archean crust (southeast Greenland). We would anticipate that the thick crust would require a substantial period to thin sufficiently to allow asthenospheric upwelling
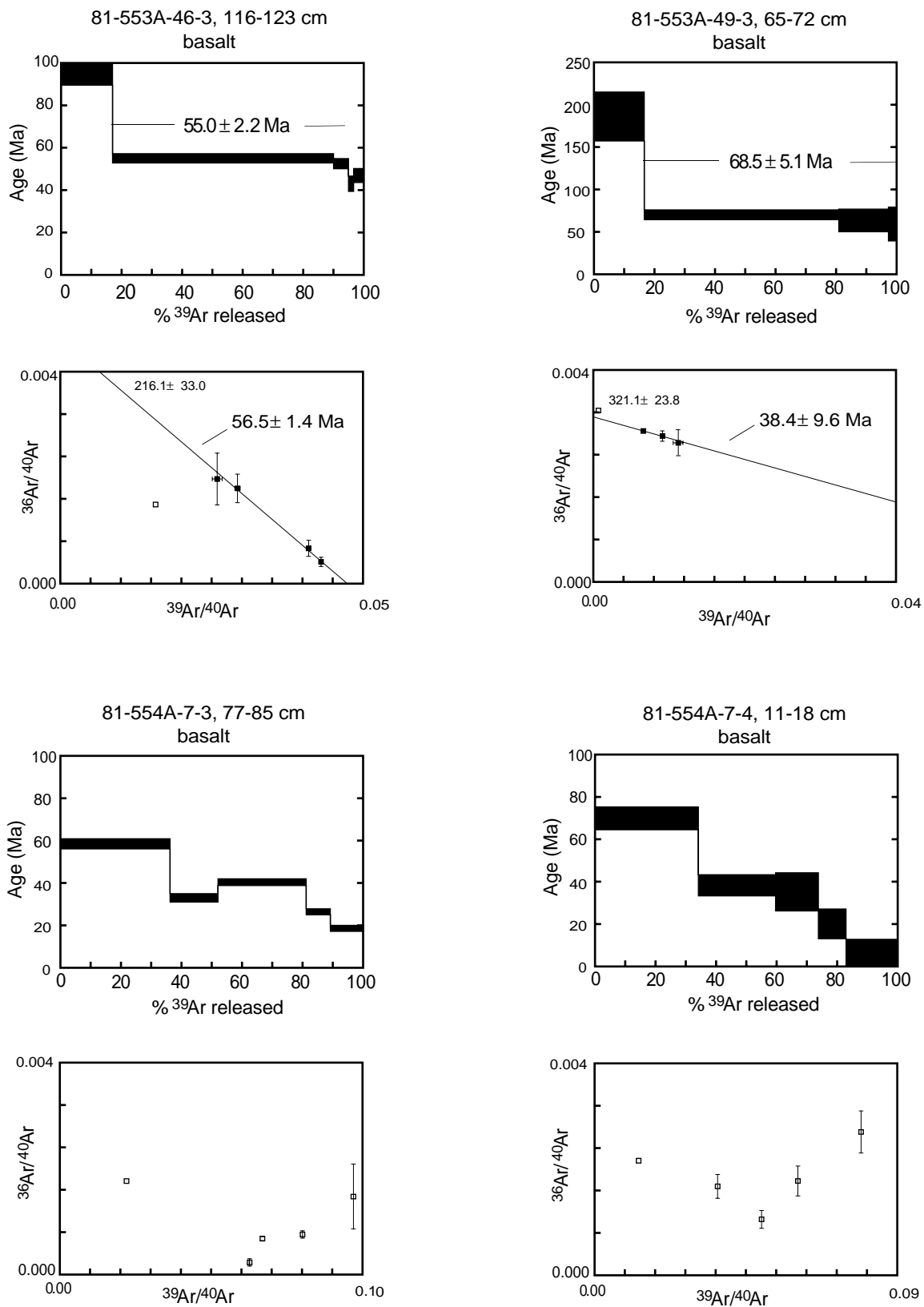
Figure 6. Step age spectra and isotope correlation diagrams from ^{40}Ar-^{39}Ar incremental heating experiments for DSDP Leg 81. The thickness of the bar for each step age in the age spectrum indicates the 2σ analytical uncertainty in age.

81-555-69-3, 121-129 cm
Hatton Bank basalt

57.6 ± 1.3 Ma

365.2 ± 10.8

51.6 ± 9.0 Ma

81-555-90-2, 102-109 cm
Hatton Bank basalt
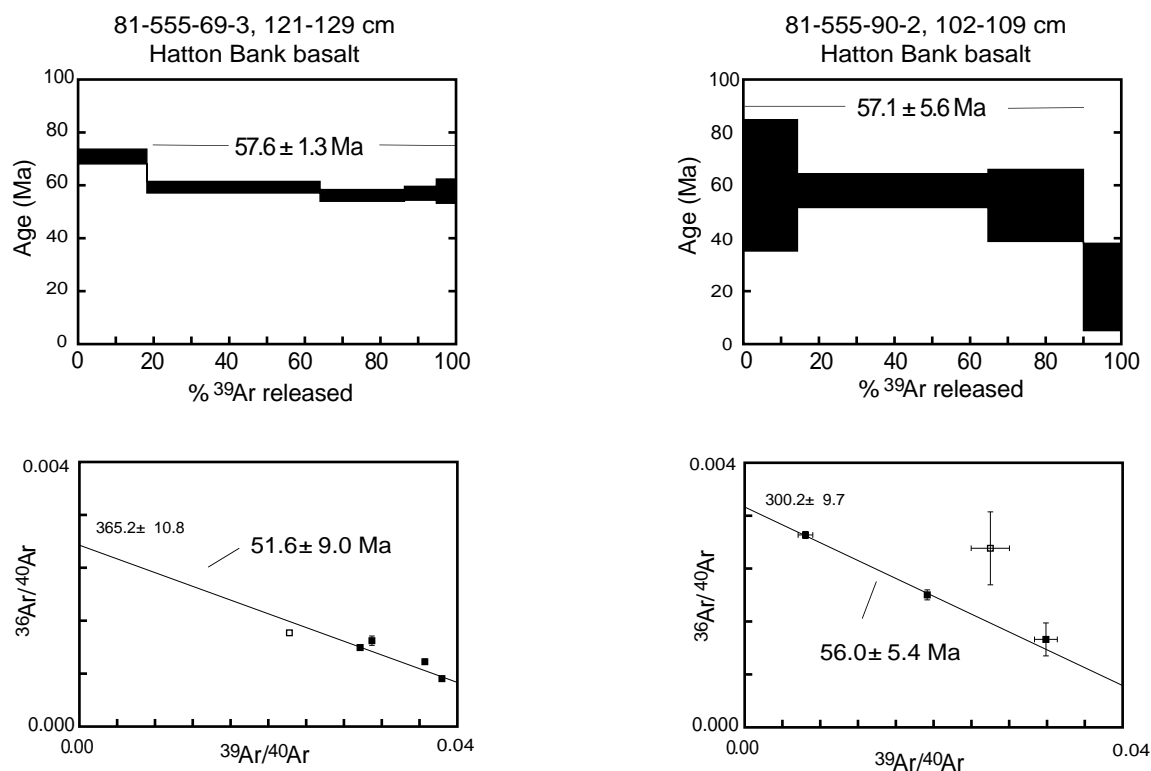
57.1 ± 5.6 Ma

300.2 ± 9.7

56.0 ± 5.4 Ma

Figure 6 (continued).

and melting. Therefore, the plume incubation model is not consistent with widespread, pre-rift initial volcanism. A third model asserts that a steady-state Iceland mantle plume existed prior to 62 Ma and that the differences in the timing of volcanism (i.e., earlier volcanism in West Greenland relative to East Greenland) are caused by plate motion over the hot spot (Lawver and Müller, 1994). This is inconsistent with widespread (at least 2000 km broad) volcanic centers at 62–61 Ma if the Iceland plume was similar to its present size.

The initial magmatic pulse was limited by the thick continental lithosphere, which could have acted as a cap at 62 Ma and prevented initially larger extents of partial melting and volcanism (e.g., Fram and Lesher, 1993). It was not until continental separation allowed upwelling of the mantle (much of it part of the hot plume head) that the second phase of magmatism occurred (White and McKenzie, 1989). This second phase of magmatism was more extensive than the initial pulse and was centralized along the present margins of the North Atlantic.

White (1992) suggested that the northwest-southeast line between West Greenland and northern Britain indicated that the initial plume had the form of a rising sheet. The new data support a general northwest-southeast trend of initial volcanism, but if the plume were a sheet of rising mantle, it was thick and irregularly shaped. Without information about the timing of the initial volcanism in other parts of the NAVP, an analysis of the shape and extent of the initial plume cannot be determined.

CONCLUSIONS

Volcanism at the southeast Greenland Margin began by 61–62 Ma with the eruption of continentally contaminated lavas. After an apparent hiatus, volcanism resumed with the eruption of lavas with negligible crustal contamination and a more MORB-like composition. Similar oceanic lavas from the southwest Rockall Plateau, which are just south of the conjugate margin to southeast Greenland, gave imprecise ages of 57–58 Ma. The apparent hiatus in volcanism

appears to be widespread in the NAVP, and it is probable that the bulk of the province was formed during two distinct magmatic episodes. The 61–62 Ma initial age of volcanism for the southeast Greenland Margin is similar to the age of the older lavas on West Greenland and northwest Britain. We associate this early stage of widespread volcanism with the arrival of the Iceland mantle plume. The later lavas of the SDRS and East Greenland began to erupt at about 57 Ma during plate separation and are the result of lithospheric thinning and creation of oceanic lithosphere from upwelling of anomalously hot asthenospheric mantle.

REFERENCES

Berggren, W.A., Kent, D.V., Flynn, J.J., and Van Couvering, J.A., 1985. Cenozoic geochronology. *Geol. Soc. Am. Bull.,* 96:1407–1418.

Berggren, W.A., Kent, D.V., Swisher, C.C., III, and Aubry, M.-P., 1995. A revised Cenozoic geochronology and chronostratigraphy. *In* Berggren, W.A., Kent, D.V., and Hardenbol, J. (Eds.), *Geochronology, Time Scales and Global Stratigraphic Correlation: A Unified Temporal Framework for an Historical Geology.* Spec. Publ.—Soc. Econ. Paleontol. Mineral., 54.

Boulter, M.C., and Manum, S.B., 1989. The Brito-Arctic igneous province flora around the Paleocene/Eocene boundary. *In* Eldholm, O., Thiede, J., Taylor, E., et al., *Proc. ODP, Sci. Results,* 104: College Station, TX (Ocean Drilling Program), 663–680.

Bridgwater, D., Keto, L., McGregor, V.R., and Myers, J.S., 1976. Archaean gneiss complex of Greenland. *In* Escher, A., and Watt, W.S. (Eds.), *Geology of Greenland:* Copenhagen (Geol. Surv. Greenland), 18–75.

Brown, S., and Downie, C., 1984. Dinoflagellate cyst biostratigraphy of late Paleocene and early Eocene sediments from Holes 552, 553A, and 555, Leg 81, Deep Sea Drilling Program (Rockall Plateau). *In* Roberts, D.G.,

Schnitker, D., et al., *Init. Repts. DSDP,* 81: Washington (U.S. Govt. Printing Office), 565−579.

Chalmers, J.A., 1991. New evidence on the structure of the Labrador Sea/Greenland continental margin. *J. Geol. Soc. London,* 148:899−908.

Dagley, P., and Mussett, A. E., 1986. Paleomagnetism and radiometric dating of the British Tertiary Igneous province: Muck and Eigg. *Geophys. J. R. Astron. Soc.,* 85:221−242.

Dalrymple, G.B., Clague, D.A., Vallier, T.L., and Menard, H.W., 1987. ^{40}Ar/^{39}Ar age, petrology, and tectonic significance of some seamounts in the Gulf of Alaska. *In* Keating, B.H., Fryer, P., Batiza, R., and Boehlert, G.W. (Eds.), *Seamounts, Islands and Atolls.* Geophys. Monogr., Am. Geophys. Union, 43:297−315.

Duncan, R.A., and Hargraves, R.B., 1990. ^{40}Ar/^{39}Ar geochronology of basement rocks from the Mascarene Plateau, the Chagos Bank, and the Maldives Ridge. *In* Duncan, R. A., Backman, J., Peterson, L.C., et al., *Proc. ODP, Sci. Results,* 115: College Station, TX (Ocean Drilling Program), 43−51.

Duncan, R.A., and Hogan, L.G., 1994. Radiometric dating of young MORB using the ^{40}Ar−^{39}Ar incremental heating method. *Geophys. Res. Lett.,* 21:1927−1930.

Eldholm, O., and Grue, K., 1995. North Atlantic volcanic margins: dimensions and production rates. *J. Geophys. Res.,* 99:2955−2968.

Eldholm, O., Thiede, J., Taylor, E., et al., 1987. *Proc. ODP, Init. Repts.,* 104: College Station, TX (Ocean Drilling Program).

Fram, M.S., and Lesher, C.E., 1993. Geochemical constraints on mantle melting during creation of the North Atlantic basin. *Nature,* 363:712−715.

Hansen, H., Rex, D.C., Guise, P.G., and Brooks, C.K., 1993. ^{40}Ar/^{39}Ar ages on Tertiary East Greenland basalts from the Scoresby Sund area. *Eos,* 74:625.

Harrison, R.K., and Merriman, R.J., 1984. Petrology, mineralogy, and chemistry of basaltic rocks: Leg 81. *In* Roberts, D.G., Schnitker, D., et al., *Init. Repts. DSDP,* 81: Washington (U.S. Govt. Printing Office), 743−774.

Hinz, K., 1981. A hypothesis on terrestrial catastrophes: wedges of very thick oceanward dipping layers beneath passive margins: their origin and paleoenvironmental significance. *Geol. Jahrb.,* E22:3−28.

Joron, J.L., Bougault, H., Maury, R.C., Bohn, M., and Desprairies, A., 1984. Strongly depleted tholeiites from the Rockall Plateau margin, North Atlantic: geochemistry and mineralogy. *In* Roberts, D.G., Schnitker, D., et al., *Init. Repts. DSDP,* 81: Washington (U.S. Govt. Printing Office), 783−794.

Jürgensen, T., and Mikkelsen, N., 1974. Coccoliths from volcanic sediments (Danian) in Nugssuaq, West Greenland. *Bull. Geol. Soc. Den.,* 23:225−230.

Kharin, G.N., Udintsev, G.B., Bogatikov, O.A., Dmitriev, J.I., Raschka, H., Kreuzer, H., Mohr, M., Harre, W., and Eckhardt, F.J., 1976. K/Ar age of the basalts of Norwegian-Greenland Sea, DSDP Leg 38. *In* Talwani, M., Udintsev, G., et al., *Init. Repts. DSDP,* 38: Washington (U.S. Govt. Printing Office), 755−759.

Knox, R.W., and Morton, A.C., 1988. The record of early Tertiary N Atlantic volcanism in sediments of the North Sea Basin. *In* Morton, A.C., and Parson, L.M. (Eds.), *Early Tertiary Volcanism and the Opening of the Northeast Atlantic.* Geol. Soc. Spec. Publ. London, 39:407−419.

Lanphere, M.A., and Dalrymple, G.B., 1976. Identification of excess ^{40}Ar by the ^{40}Ar/^{39}Ar age spectrum technique. *Earth Planet. Sci. Lett.,* 32:141−148.

————, 1978. The use of ^{40}Ar/^{39}Ar data in evaluation of disturbed K-Ar systems. *In* Zartman, R.E. (Ed.), *Short Papers of the Fourth International Conference, Geochronology, Isotope Geology.* Open-File Rep.—U.S. Geol. Surv., 78-701:241−243.

Lanphere, M.A., Dalrymple, G.B., Fleck, R.J., and Pringle, M.S., 1990. Intercalibration of mineral standards for K-Ar and ^{40}Ar-^{39}Ar age measurements. *Eos,* 71:1658.

Larsen, H.C., and Jakobsdóttir, S., 1988. Distribution, crustal properties and significance of seaward-dipping sub-basement reflectors off East Greenland. *In* Morton, A.C., and Parson, L.M. (Eds.), *Early Tertiary Volcanism and the Opening of the Northeast Atlantic.* Geol. Soc. Spec. Publ. London, 39:95−114.

Larsen, H.C., Saunders, A.D., Clift, P.D., et al., 1994. *Proc. ODP, Init. Repts.,* 152: College Station, TX (Ocean Drilling Program).

Larsen, L.M., Pedersen, A.K., Pedersen, G.K., and Piasecki, S., 1992. Timing and duration of Early Tertiary volcanism in the North Atlantic: new evidence from West Greenland. *In* Storey, B.C., Alabaster, T., and Pankhurst, R.J. (Eds.), *Magmatism and the Causes of Continental Breakup.* Geol. Soc. Spec. Publ. London, 68:321−333.

Lawver, L.A., and Müller, R.D., 1994. Iceland hotspot track. *Geology,* 22:311−314.

LeHuray, A.P., and Johnson, E.S., 1989. Rb-Sr systematics of Site 642 volcanic rocks and alteration minerals. *In* Eldholm, O., Thiede, J., Taylor, E., et al., *Proc. ODP, Sci. Results,* 104: College Station, TX (Ocean Drilling Program), 437−448.

Macintyre, R.M., and Hamilton, P.J., 1984. Isotopic geochemistry of lavas from Sites 553 and 555. *In* Roberts, D.G., Schnitker, D., et al., *Init. Repts. DSDP,* 81: Washington (U.S. Govt. Printing Office), 775−781.

Morton, A.C., Evans, D., Harland, R., King, C., and Ritchie, D.K., 1988. Volcanic ash in a cored borehole W of the Shetland Islands: evidence for Selandian (late Paleocene) volcanism in the Faeroes region. *In* Morton, A.C., and Parson, L.M. (Eds.), *Early Tertiary Volcanism and the Opening of the NE Atlantic.* Geol. Soc. Spec. Publ. London, 263−269.

Mussett, A.E., 1986. ^{40}Ar-^{39}Ar step-heating ages of the Tertiary igneous rocks of Mull, Scotland. *J. Geol. Soc. London,* 143:887−896.

Mussett, A.E., Dagley, P., and Skelhorn, R.R., 1988. Time and duration of activity in the British Tertiary Igneous Province. *In* Morton, A.C., and Parson, L.M. (Eds.), *Early Tertiary Volcanism and the Opening of the NE Atlantic.* Geol. Soc. Spec. Publ. London, 337−348.

Noble, R.H., Macintyre, R.M., and Brown, P.E., 1988. Age constraints on Atlantic evolution: timing of magmatic activity along the E Greenland continental margin. *In* Morton, A.C., and Parson, L.M. (Eds.), *Early Tertiary Volcanism and the Opening of the North Atlantic.* Geol. Soc. Spec. Publ. London, 201−214.

Pearson, D.G., Emeleus, C.H., and Kelley, S.P., 1996. Precise ^{40}Ar/^{39}Ar age for the initiation of Palaeogene volcanism in the Inner Hebrides and its regional significance. *J. Geol. Soc. London,* 153:815−818.

Perch-Nielsen, K., 1973. Danian and Campanian/Maastrichtian coccoliths in a volcanic province, West Greenland. *Bull. Geol. Soc. Den.,* 22:79−82.

Richards, M.A., Duncan, R.A., and Courtillot, V.E., 1989. Flood basalts and hot-spot tracks: plume heads and tails. *Science,* 246:103−107.

Richardson, C., Oakley, P.J., and Cann, J.R., 1984. Trace and major element chemistry of basalts from Leg 81. *In* Roberts, D.G., Schnitker, D., et al., *Init. Repts. DSDP,* 81: Washington (U.S. Govt. Printing Office), 795−806.

Roberts, D.G., Schnitker, D., et al., 1984. *Init. Repts. DSDP,* 81: Washington (U.S. Govt. Printing Office).

Schönharting, G., and Abrahamsen, N., 1989. Paleomagnetism of the volcanic sequence in Hole 642E, ODP Leg 104, Vøring Plateau, and correlation with early Tertiary basalts in the North Atlantic. *In* Eldholm, O., Thiede, J., Taylor, E., et al., *Proc. ODP, Sci. Results,* 104: College Station, TX (Ocean Drilling Program), 911−920.

Storey, M., Duncan, R.A., Pedersen, A.K., Larsen, L.M., and Larsen, H.C., in press. ^{40}Ar-^{39}Ar geochronology of the West Greenland Tertiary volcanic province.

Talwani, M., and Eldholm, O., 1977. Evolution of the Norwegian-Greenland Sea. *Geol. Soc. Am. Bull.,* 88:969−999.

Talwani, M., Udintsev, G., et al., 1976. *Init. Repts. DSDP,* 38: Washington (U.S. Govt. Printing Office).

Taylor, P.N., and Morton, A.C., 1989. Sr, Nd, and Pb isotope geochemistry of the upper and lower volcanic series at Site 642. *In* Eldholm, O., Thiede, J., Taylor, E., et al., *Proc. ODP, Sci. Results,* 104: College Station, TX (Ocean Drilling Program), 429−435.

Thompson, R.N., and Gibson, S.A., 1991. Subcontinental mantle plumes, hotspots and pre-existing thinspots. *J. Geol. Soc. London,* 147:973−977.

Upton, B.G.J., Emeleus, C.H., Rex, D.C., and Thirlwall, M.F., 1995. Early Tertiary magmatism in NE Greenland. *J. Geol. Soc. London,* 152:959−964.

Vogt, P.R. and Avery, O.E., 1974. Detailed magnetic surveys in the northeast Atlantic and Labrador Sea. *J. Geophys. Res.,* 79:363−389.

White, R.S., 1992. Magmatism during and after continental breakup. *In* Storey, B.C., Alabaster, T., and Pankhurst, R.J. (Eds.), *Magmatism and the Causes of Continental Breakup.* Geol. Soc. Spec. Publ. London, 1−16.

White, R.S., and McKenzie, D., 1989. Magmatism at rift zones: the generation of volcanic continental margins and flood basalts. *J. Geophys. Res.,* 94:7685−7729.
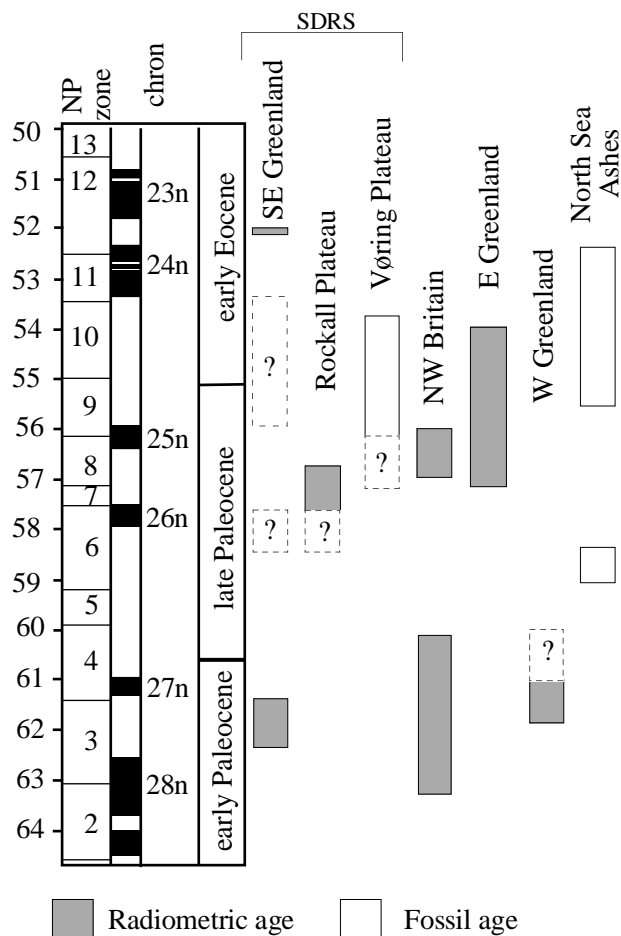
Figure 7. Compilation of new radiometric ages presented in this paper and published ages from West Greenland (Larsen et al., 1992), East Greenland (Noble et al., 1988; Hansen et al., 1993; Upton et al., 1995), northwest Britain (Dagley and Mussett, 1986; Mussett, 1986), the Vøring Plateau (Boulter and Manum, 1989), and North Sea sediments (Knox and Morton, 1988; Morton et al., 1988). We cannot discount older ages in the eastern Atlantic SDRS because the lower lavas were not sampled. The dashed range near 57 Ma for the southeast Greenland SDRS represents our inferred age for the oceanic lava series. The magnetic and numerical time scale is from Berggren et al. (1995), and the NP zones are from Berggren et al. (1985).